Available online at www.sciencedirect.com
SCIENCE DIRECT
Neuroscience Research 52 (2005) 132–138
Neuroscience Research
www.elsevier.com/locate/neures

Update article

Large-scale imaging of cortical network activity with calcium indicators

Yuji Ikegaya *, Morgane Le Bon-Jego, Rafael Yuste

Department of Biological Sciences, Columbia University, 1002 Fairchild Center, M.C. 2435 New York, NY 10027, USA

Received 18 February 2005; accepted 21 February 2005
Available online 17 March 2005

Abstract

Bulk loading of calcium indicators has provided a unique opportunity to reconstruct the activity of cortical networks with single-cell resolution. Here we describe the detailed methods of bulk loading of AM dyes we developed and have been improving for imaging with a spinning disk confocal microscope.

Keywords: Slice preparation; Cortex; Fluo-4; Oregon green; Spike; Microcircuitry; Action potential; Circuit; Spinning disk confocal microscope

1. Introduction

Sound, light, tactile, taste and odor stimuli are all translated into neural signals. The brain processes this information using neurons, synapses and neural networks. At the same time, the brain is constantly active; even in the absence of sensory stimuli, neurons are continuing to emit spikes from before birth until death. These evoked and spontaneous activities are both based on the intrinsic properties of neurons and on circuit mechanisms. In this sense, our understanding of the brain must arise from the comprehension of the function and structure of the circuits woven by numerous neurons. This is attainable, al least in part, with large-scale recordings of neuronal activity, a method that allows us to observe the temporal and spatial patterns of firing activity of neuron population.

Such large-scale monitoring of neuronal activity includes electroencephalogram (EEG), functional magnetic resonance imaging (fMRI), positron emission tomography (PET), multiple-unit recordings with stereotrodes, and optical imaging with voltage-sensitive dyes. However, these procedures have not allowed recording with strict single-cell resolution so far.

To circumvent these problems, we developed a method for bulk loading cortical slices with acetoxymethyl (AM) esters of fluorescent calcium indicators (Yuste and Katz, 1991). The AM-ester dyes are up-taken by living cells, hydrolyzed by the intracellular esterase activity and become an active form only inside the cells. An idea is that neurons in a brain slice are labeled with calcium indicators through uptake of the AM-ester forms in order to detect action potential-relevant calcium transients in the somata simultaneously from a large population of neurons. This method enables recordings with single-cell resolution and post-hoc histological reconstruction of neurons. At present this is the only technique by which action potentials can be monitored simultaneously from thousands of neurons (Cossart et al., 2003; Ikegaya et al., 2004; Ohki et al., 2005). Moreover, this procedure is applicable to imaging of calcium oscillations in astrocyte populations (Tashiro et al., 2002; Nett et al., 2002; Morita et al., 2003; Liu et al., 2004; Sul et al., 2004). Here we describe the experimental procedures of bulk loading and its application and limitation.

* Corresponding author. Present address: Laboratory of Chemical Pharmacology, Graduate School of Pharmaceutical Sciences, The University of Tokyo, 7-3-1 Hongo, Bunkyo-ku, Tokyo 113-0033, Japan. Tel.: +1 212 854 2354/81 3 5841 4784; fax: +1 212 865 8246/81 3 5841 4784.
E-mail addresses: ikegaya@tk.air.jp, ikegaya@tk.airnet.ne.jp, yi2109@columbia.edu (Y. Ikegaya), mjego@biology.columbia.edu (M. Le Bon-Jego).

0168-0102/$ – see front matter
doi:10.1016/j.neures.2005.02.004

2. Slice preparations

The patterns of neural activity in slice preparations are affected by a number of experimental conditions, e.g., species, age, slicing angle, temperature, ionic composition of artificial cerebrospinal fluid (aCSF), etc. The thickness of slices is also a critical factor; an only 100 μm increase in the thickness of a rat cortical slice is known to lead to a few-fold increase in the average probability of an interneuron innervating pyramidal neurons (Thomson et al., 1996). It is also noteworthy that the mouse cortex is smaller than that of the rat and that the neurons in the mouse cortex are more densely packed. Thus, if one makes brain slices at the same thickness, the cortical microcircuit in mice is much more intact in the slice than in rats.

We usually use 350 μm-thick slices from postnatal day 14 C57Bl/6 mice. Animals are anaesthetized with 100 mg/kg ketamine and 5 mg/kg xylazine (i.p.) and sacrificed by decapitation, and the brains are rapidly removed and transferred into ice-cold aCSF (123 mM NaCl, 3 mM KCl, 26 mM $NaHCO_3$, 1 mM NaH_2PO_4, 2 mM $CaCl_2$, 1.5 mM $MgSO_4$ and 10 mM dextrose). Coronal slices are cut with a Leica VT1000S vibratome in ice-cold sucrose solution bubbled with 95% O_2 and 5% CO_2. To prevent cell damages, we cut slices in a modified solution that consists of: 222 mM sucrose, 2.6 mM KCl, 27 mM $NaHCO_3$, 1.5 mM NaH_2PO_4, 0.5 mM $CaCl_2$, 7 mM $MgSO_4$, and 0.1 mM ascorbic acid. The slices are maintained in aCSF at room temperature for 30–45 min and then loaded with calcium indicators.

3. Bulk loading with calcium indicators

Loading methods for fluorescent indicators excited with UV light such as fura-2AM (Molecular Probes) has been described elsewhere (Yuste and Katz, 1991; Smetters et al., 1999; McLean and Yuste, 2005). In this article, we would rather focus on visible light-excited dyes, including fluo-4 and Oregon green derivatives (Molecular Probes). Non-UV-excitation causes a fewer degree of cell damages and can work with a conventional, less expensive confocal microscope.

In order to load neurons with calcium indicators, four slices are placed on the porous membrane (pore size 0.4 μm) of a Millicell-CM culture transwell (PICM 03050, 30 mm diameter) which is inserted into a 35 mm dish. Both the inside and outside of the transwell are filled with 1 ml of aCSF. The 3 μl of a dye solution is then dropped onto the top of each individual slice so that the slice is initially exposed to a high concentration of the AM dye (Fig. 1A). This dye solution is prepared by adding 48 μl DMSO and 2 μl Pluronic F-127 (10% solution in DMSO, P-6866, Molecular Probes) into a tube of 50 μg fluo-4 AM (F-14201, special package, Molecular Probes) or 50 μg Oregon green 488 BAPTA-1 AM (O-6807, special package, Molecular Probes). Thus, the dye solution finally contains 0.1% (∼1 mM) AM-ester dye and 0.4% Pluronic F-127 in DMSO.

The incubation is performed in the dark at 37 °C for 15 min (fluo-4AM) or 40–45 min (Oregon green 488 BAPTA-1 AM) during which 95% O_2 and 5% CO_2 is continuously supplied under moist conditions. The loading is terminated by transferring the slices into fresh aCSF. The slices are maintained at room temperature for at least 30 min before imaging.

Another method for bulk loading utilizes Cremophor EL (C5135, Sigma) as well as Pluronic F-127. These reagents are both detergents known to facilitate the solubilization of water-insoluble dyes, and they may have cellular toxicity, so they should be used at as low concentrations as possible unless the efficacy is reduced. The 50 μg Oregon green 488 BAPTA-1 AM (special package, Molecular Probes) is dissolved in 8 μl of 0.5% Cremophor EL/DMSO and 2 μl of 10% Pluronic F-127/DMSO, and then added to 2 ml aCSF. Thus, the final concentrations are 0.0025% (∼20 μM) for AM-ester dye, 0.002% Cremophor EL, 0.01% Pluronic F-127 and 0.5% DMSO. In this solution, slices are kept in the dark at 37 °C for 40–45 min (Fig. 1B). The technique using Cremophor EL is more efficient and consistent than that with Pluronic F-127 alone. In the presence of Cremophor EL, calcium indicators label as many as 93.2 ± 7.5% cells (mean ± S.D., layer 2/3 of P14 mouse prefrontal cortex, $n = 4$ slices), as compared visually with differential interference contrast (DIC) images (Fig. 1C). This proportion, however, seems to decrease with increasing ages of animal (Peterlin et al., 2000; but see for in vivo experiments, Stosiek et al., 2003). In general, superficial layers tend to show a higher labeling efficiency, and in particular, fluo-4 AM hardly labels layer 5 pyramidal cells even in P14 mouse slices, presumably because the superficial layers contain the most recently post-migratory neurons. Consistent with this, the dentate gyrus developed later than the hippocampus, and dentate granule cells are more easily labeled with AM dyes than hippocampal pyramidal cells. We have carefully compared and improved the techniques of loading, and now consider that the most efficient loading is obtained with Oregon green 488 BAPTA-1 AM using Cremophor EL protocol (93.2 ± 7.5% cells labeled with Oregon green 488 BAPTA-1 with Cremophor EL; at most 60% cells labeled without Cremophor EL).

4. Confocal imaging

High-speed time-lapse imaging is desired to reconstruct the precise pattern of spike-relevant events. The spinning disk confocal microscope uses a multiple pinhole mast, a so-called Nipkow disk, in an intermediate image plane to scan numerous illumination points over the specimen without moving the light source or microscope stage. This confocal is capable of acquiring images at a rate of up to 300 frames/s, allowing fast imaging of living cells (the actual data-acquiring

speed is limited by the capability of a CCD camera). We use a Perkin Elmer UltraView spinning disk confocal microscope with an Olympus BX50 upright microscope and a Hamamatsu ORCA-ER CCD camera. With an Olympus 10× and 20× water immersion objectives, we scan areas of 896 μm × 683 μm and 448 μm × 341 μm, respectively, with 672 × 512 pixels (2 × 2 binning). One pixel is 1.8 μm^2 (10×) and 0.45 μm^2 of area (20×), and thus it is enough larger than the size of the soma of a neuron. Frame rates are typically at 5–10 frames/s, and the file size of one frame is approximately 673 KB in a 16-bit tiff format, and thus, the total file size of a movie grows up to a few GB for minutes, requiring a large data storage system.

5. Signal extractions

All frames of a movie are collapsed into a single image by averaging fluorescence intensity with the max-intensity mode of Z-projection stacking in the free software Image J (National Institutes of Health). The following processes are all performed with custom-made codes in Image J (National Institutes of Health) and Matlab (MathWorks), some of which algorism are under patent application. The intensity in a stacked image is spatially normalized using a 12 × 12 pixel localizing filter, in which each pixel value is divided by the mean value of a 12 × 12 pixel surround. Cell contours are automatically detected by finding contiguous regions of at least 15-$pixel^2$ area where all pixels are brighter than a threshold level. The averaged fluorescence of the pixels inside each contour is read in each frame of the movie.

To detect individual optical events, the baseline of each trace is calculated by smoothing the trace with the Hamming filter for a time window of 300–600 ms, and the fluorescence change over time is defined as $\Delta F/F = (F - F_{basal})/F_{basal}$, where F is the fluorescence at any time point, and F_{basal} the baseline fluorescence averaged across the whole movie for each cell. In our experimental conditions, the bleach rate of fluorescence is approximately 1%/min. The rising phases of calcium transients correspond with spiking time as assessed by simultaneous intracellular recording (Fig. 1D), and we

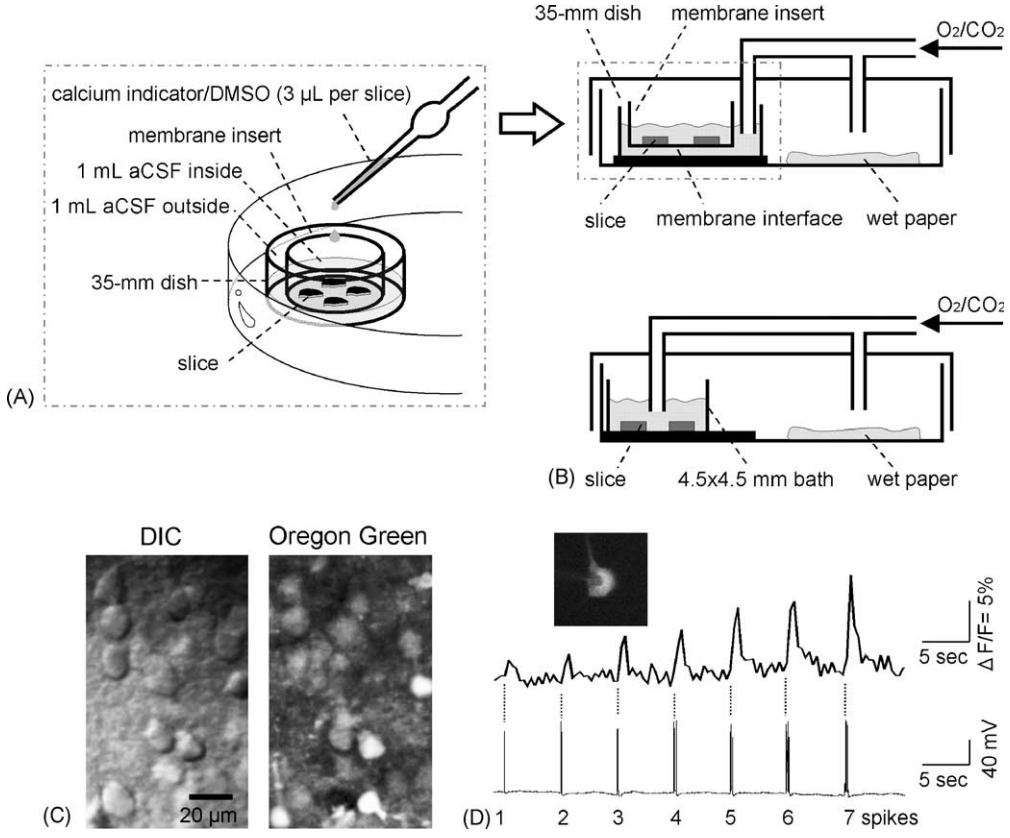

Fig. 1. Loading of neuronal populations with calcium indicators in cortical slices. (A) and (B) Schematic draws of loading chambers. In the pseudo-double incubation protocol (A), a high concentration of an AM-ester dye is dropped onto the surface of each slice, and it is gradually diluted through passive diffusion. In the one step protocol (B), slices are immersed in a relatively low concentration (typically 10 μM) of dye solution. For details, see text. (C) DIC image (left) and fluorescence photomicrograph (right) of Oregon green 488 BAPTA-1 AM in the same field of a coronal slice from P14 mouse prefrontal cortex. The field encompasses layer 2/3 with the pial surface to the top. (D). Representative fluorescence trace (top) and simultaneous intracellular recording (bottom) of a layer 2/3 pyramidal neuron from P15 mouse loaded with 25 μM Oregon green 488 BAPTA-1 in the pipette (inset). Calcium transient sizes in the soma are associated with the numbers of spikes. The numbers below the intracellular trace indicate the numbers of evoked spikes.

thus reconstruct spike timings of the cells by thresholding the first derivative of fluorescence changes (Smetters et al., 1999). The derivative is determined by the slope between the endpoints of a 0.5–1.0 s cursor.

To estimate the amount of noise, we carried out extra-experiments for calibration in which we monitored baseline in the presence of either 1 μM tetrodotoxin or 2 mM Ni^{2+} to block spike-relevant calcium events, and measure the standard deviation (S.D.) of the values of all points above the baseline in first derivative. Cd^{2+} can also be used to block high threshold voltage-gated calcium currents. Each action potential during high-frequency firing cannot be detected because the calcium signals at our time resolution are not sufficiently greater than noise to be resolved (Smetters et al., 1999). For that reason we focus only on the onsets of calcium transients, which represent the initiation of burst discharges. Such onset events are marked as start timings of calcium transients at which the first derivative trace exceeds 2.58 S.D. of noise (the 1% point of the Gaussian distribution). This threshold was determined by the above calibration experiments. Neurons were loaded with 25 μM Oregon green 488 BAPTA-1 in the pipette. One action potential is able to produce a calcium transient above the threshold, but obviously, a calcium transient produced by a burst discharge are easier to detect because of the larger size (Fig. 1D). Finally, we verify all automatically detected events by examining raw traces of brightness (not $\Delta F/F$) by eye and manually reject any falsely detected "events". Spike-related events are easily distinguishable from noise since spikes are followed by calcium decays over hundreds of milliseconds and also because the local peak of $\Delta F/F$ is usually larger than 1.5% (Figs. 1D and 2A).

6. Neuronal signal and glial signal

Fluo-4 AM and Oregon green 488 BAPTA-1 AM label glia as well as neurons. Therefore, signals extracted by the above procedure may be contaminated with glial calcium waves. Although the discrimination of neurons from glia in living slices is a hard problem, there are several possible ways to do it:

(1) In most cases, glial cells are much strongly labeled in the absolute fluorescence intensity, as compared to neurons (Fig. 2A). Because the resting calcium level in glia is similar to or even slightly lower than that in neurons (Beck et al., 2004), we consider that glia may have a higher ability to uptake or hydrolyze AM-ester dyes. Owing to this fact, we can often see the shape of glia. Glial cells bear several foot processes that are shorter and much thicker than neurites. Thus the cell morphology can help discriminate neurons from glia. To do this precisely, higher magnification (20× and more objective) should be used for imaging.

(2) Temporal profiles of calcium transients are another guide for cell identification. Glia usually show slow kinetics of calcium signals (Fig. 2A, see also Tashiro et al., 2002; Badea et al., 2001), although there are occasional exceptions. Intracellular calcium in glia

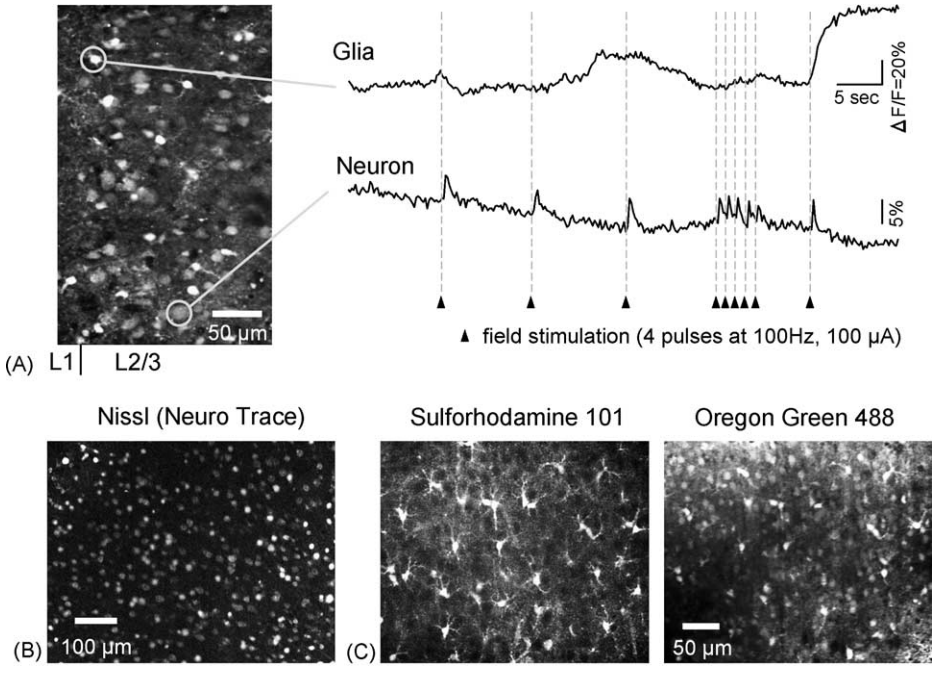

Fig. 2. Discrimination of neurons and glia. (A) Glial cells are labeled by Oregon green 488 BAPTA-1 AM more strongly than neurons, and its calcium signal has a slow kinetics and large amplitude. Note the vertical scales in the right panels. (B) and (C) The red fluorescent dyes Nissl and sulforhodamine 101 preferentially label neurons and glia in living cortical slices, respectively.

typically rises in the order of a seconds and decreases in the order of tens of seconds. In some cases, the elevated calcium level persists for a few minutes. In contrast, neuronal calcium increases sharply (typically within one movie frame) and decreases in the order of hundreds of milliseconds (Figs. 1D and 2A). In addition, the amplitude of glial calcium transients is usually larger than that of neurons (Fig. 2A). Unlike neuronal signals, Glial signals tend to be oscillatory but they are not temporally correlated in a population (Fig. 3, see also Nett et al., 2002; Tashiro et al., 2002).

(3) The physiological proprieties of calcium signals are also different between neurons and glia. Neurons rapidly respond to an electric stimulus of afferent fibers with fast calcium transients, but glia responds sluggishly or is often irresponsive (Fig. 2A). Glial signals occur even in the presence of tetrodotoxin (Badea et al., 2001; Tashiro et al., 2002).

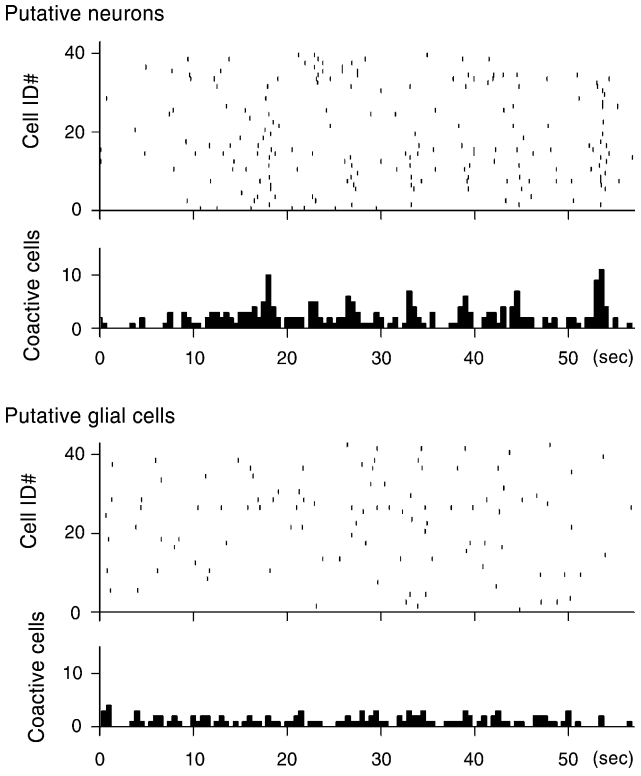

Fig. 3. Spontaneous activity of neurons and glial cells. Neurons and glia are separated based on the morphology and baseline fluorescence intensity of fluo-4 labeled cells, and the kinetics of calcium transients (see text). In this movie, forty putative neurons and 43 putative glial cells showed calcium transients. Each top panel indicates a spatiotemporal pattern in the activity of individual cells, each onset time of which is shown as a dot in the rasterplot. The cell order, i.e., the ordinate, was arbitrarily sorted to see temporal correlations well. The bottom histograms represent the numbers of coactive cells with a time bin of 500 ms, indicating that population activity yields occasional synchronization among neurons, but not glia. The level of this synchrony, which we call "cortical flash," cannot be accounted for by chance, as assessed by a modified Monte Carlo simulation (see Cossart et al., 2003).

(4) Another strategy is the use of cell type-specific dyes that are available in living cells. We are using NeuroTrace™ 530/615 fluorescent Nissl stain (N-21482, Molecular Probes) and sulforhodamine 101 (S-359, Molecular Probes). The former is considered a marker specific to neurons (Rao et al., 2003) and the latter specific to astrocytes (Nimmerjahn et al., 2004) at least in the cortex. Both dyes emit red florescence and can be combined with bulk loading with green fluorescent calcium indicators (Ikegaya et al., 2004; Nimmerjahn et al., 2004). For Nissl staining, we dissolve 50 μg fluo-4 AM with 23 μl Nissl, 2 μl Pluronic F-127 and 25 μl DMSO and incubate cortical slices in this dye solution as described above (Fig. 1A). Nissl fluorescence is not very strong in intensity, and hence, a longer exposure time of camera is required to take fine images as compared with fluo-4 (Fig. 2B). Nissl staining sometimes (but not always) might decrease the level of spontaneous network activity. Moreover, Nissl dye is unlikely able to stain all neurons present in a slice in our experimental conditions, although the ratio of labeled neurons is >50% (Fig. 2B). Recently we also have started to use sulforhodamine 101. We employ the protocol developed in vivo by Nimmerjahn et al. (2004) for labeling astrocytes. The 10 μl of 100 μM sulforhodamine 101/aCSF is directly added in the recording chamber at the end of each experiment (Fig. 2C). After at least 15 min, images are taken. Sulforhodamine 101 also requires a longer exposure time of camera to take fine images as compared with Oregon Green 488 BAPTA-1 (Fig. 2C).

(5) Finally, transgenic mouse lines that express green fluorescent protein (GFP) in a cell-type-specific manner are available. For example, transgenic mice with GFP under the control of the promoter of glial fibrillary acidic protein show astrocyte-specific GFP expression, which allows to separate astrocytic signal from others. Aguado et al. (2002) carried out bulk loading of AM-ester dyes in brain slices prepared from these transgenic mice and found that astrocytes form a complex correlated network that is synchronous with spontaneous neuronal networks.

7. Conclusions

We have reviewed our experience of bulk loading of neuron populations with the AM form of calcium indicators in cortical slices. Although this technique may be subject to several limitations as described above, it has a great potential to contribute to studies of the cortical microcircuit. Indeed we and other groups have taken advantage of this technique to reconstruct the spatial and temporal patterns of spontaneous neural firing (Mao et al., 2001; Cossart et al., 2003; Ikegaya et al., 2004), epileptic activity propagations (Badea et al., 2001), afferent stimuli-evoked events (Fig. 2A, see also Beierlein et al., 2002), neuronal

responses to chemical stimuli (Yuste and Katz, 1991), and correlated activity in the immature cortex (Yuste et al., 1992; Garaschuk et al., 2000). This technique can also be used for ''optical probing'' of neuronal circuits, a method that isolates and records from a population of neurons that trigger action potentials in simultaneously recorded, monosynaptically coupled ''follower'' neurons (Peterlin et al., 2000; Kozloski et al., 2001). The use of transgenic mice that express GFP in subpopulations of neurons, including GAD67-transgenic mouse (Oliva et al., 2000), GAD67-GFP knock-in mouse (Tamamaki et al., 2003), GAD65-GFP transgenic mouse (Lopez-Bendito et al., 2004), Kv3.1-GFP transgenic mouse (Metzger et al., 2002), and parvalbumin-GFP transgenic mouse (Meyer et al., 2002), combined with this method, would provide us with more detailed information about the organization of the microcircuit. In addition, calcium method has recently started to be applied to in vivo optical monitoring of the population activity of neurons (Stosiek et al., 2003; Nimmerjahn et al., 2004; Ohki et al., 2005) and astrocytes (Hirase et al., 2004; Nimmerjahn et al., 2004), and therefore, we are now able to address physiologically evoked neuronal responses of the cortex with single-cell resolution in vivo (Stosiek et al., 2003; Ohki et al., 2005).

Acknowledgements

We thank Andrew J. Trevelyan for his comments on the protocol of loading with sulforhodamine 101. Funded by the National Eye Institute, the University of Tokyo, and European Community's Sixth Framework Programme (Marie Curie Outgoing International Fellowships No. 2838). Parts of this text have been published in Ikegaya, Y., Aaron, G., Yuste, R. Imaging the spontaneous and evoked cortical dynamics: large-scale analysis of temporal structures of neuronal ensemble activity. *Soc. Neurosci. Short Course*. To acquire the software described here, contact Yuji Ikegaya or Morgane Le Bon-Jego.

References

Aguado, F., Espinosa-Parrilla, J.F., Carmona, M.A., Soriano, E., 2002. Neuronal activity regulates correlated network properties of spontaneous calcium transients in astrocytes in situ. J. Neurosci. 22, 9430–9444.

Badea, T., Goldberg, J., Mao, B., Yuste, R., 2001. Calcium imaging of epileptiform events with single-cell resolution. J. Neurobiol. 48, 215–227.

Beck, A., Nieden, R.Z., Schneider, H.P., Deitmer, J.W., 2004. Calcium release from intracellular stores in rodent astrocytes and neurons in situ. Cell Calcium 35, 47–58.

Beierlein, M., Fall, C.P., Rinzel, J., Yuste, R., 2002. Thalamocortical bursts trigger recurrent activity in neocortical networks: layer 4 as a frequency-dependent gate. J. Neurosci. 22, 9885–9894.

Cossart, R., Aronov, D., Yuste, R., 2003. Attractor dynamics of network UP states in the neocortex. Nature 423, 283–288.

Garaschuk, O., Linn, J., Eilers, J., Konnerth, A., 2000. Large-scale oscillatory calcium waves in the immature cortex. Nat. Neurosci. 3, 452–459.

Hirase, H., Qian, L., Bartho, P., Buzsaki, G., 2004. Calcium dynamics of cortical astrocytic networks in vivo. PLoS Biol. 2, E96.

Ikegaya, Y., Aaron, G., Cossart, R., Aronov, D., Lampl, I., Ferster, D., Yuste, R., 2004. Synfire chains and cortical songs: temporal modules of cortical activity. Science 304, 559–564.

Kozloski, J., Hamzei-Sichani, F., Yuste, R., 2001. Stereotyped position of local synaptic targets in neocortex. Science 293, 868–872.

Liu, Q.S., Xu, Q., Arcuino, G., Kang, J., Nedergaard, M., 2004. Astrocyte-mediated activation of neuronal kainate receptors. Proc. Natl. Acad. Sci. U.S.A. 101, 3172–3177.

Lopez-Bendito, G., Sturgess, K., Erdelyi, F., Szabo, G., Molnar, Z., Paulsen, O., 2004. Preferential origin and layer destination of GAD65-GFP cortical interneurons. Cereb. Cortex 14, 1122–1133.

Mao, B.Q., Hamzei-Sichani, F., Aronov, D., Froemke, R.C., Yuste, R., 2001. Dynamics of spontaneous activity in neocortical slices. Neuron 32, 883–898.

McLean, J.M., Yuste, R., 2005. Loading neocortical slices with AM indicators. In: Yuste, R., Konnerth, A. (Eds.), Imaging in Neuroscience and Development. Cold Spring Harbor Laboratory, New York, pp. 351–355.

Metzger, F., Repunte-Canonigo, V., Matsushita, S., Akemann, W., Diez-Garcia, J., Ho, C.S., Iwasato, T., Grandes, P., Itohara, S., Joho, R.H., Knopfel, T., 2002. Transgenic mice expressing a pH and Cl-sensing yellow-fluorescent protein under the control of a potassium channel promoter. Eur. J. Neurosci. 15, 40–50.

Meyer, A.H., Katona, I., Blatow, M., Rozov, A., Monyer, H., 2002. In vivo labeling of parvalbumin-positive interneurons and analysis of electrical coupling in identified neurons. J. Neurosci. 22, 7055–7064.

Morita, M., Higuchi, C., Moto, T., Kozuka, N., Susuki, J., Itofusa, R., Yamashita, J., Kudo, Y., 2003. Dual regulation of calcium oscillation in astrocytes by growth factors and pro-inflammatory cytokines via the mitogen-activated protein kinase cascade. J. Neurosci. 23, 10944–10952.

Nett, W.J., Oloff, S.H., McCarthy, K.D., 2002. Hippocampal astrocytes in situ exhibit calcium oscillations that occur independent of neuronal activity. J. Neurophysiol. 87, 528–537.

Nimmerjahn, A., Kirchoff, F., Kerr, J.N.D., Helmchen, F., 2004. Sulforhodamine 101 as a specific marker of astroglia in the neocortex. Nat. Meth. 1, 31–37.

Ohki, K., Chung, S., Ch'ng, Y.H., Kara, P., Reid, R.C., 2005. Functional imaging with cellular resolution reveals precise micro-architecture in visual cortex. Nature 433, 597–603.

Oliva Jr., A.A., Jiang, M., Lam, T., Smith, K.L., Swann, J.W., 2000. Novel hippocampal interneuronal subtypes identified using transgenic mice that express green fluorescent protein in GABAergic interneurons. J. Neurosci. 20, 3354–3368.

Peterlin, Z.A., Kozloski, J., Mao, B.Q., Tsiola, A., Yuste, R., 2000. Optical probing of neuronal circuits with calcium indicators. Proc. Natl. Acad. Sci. U.S.A. 97, 3619–3624.

Rao, S.D., Yin, H.Z., Weiss, J.H., 2003. Disruption of glial glutamate transport by reactive oxygen species produced in motor neurons. J. Neurosci. 23, 2627–2633.

Smetters, D., Majewska, A., Yuste, R., 1999. Detecting action potentials in neuronal populations with calcium imaging. Methods 18, 215–221.

Stosiek, C., Garaschuk, O., Holthoff, K., Konnerth, A., 2003. In vivo two-photon calcium imaging of neuronal networks. Proc. Natl. Acad. Sci. U.S.A. 100, 7319–7324.

Sul, J.-Y., Orosz, G., Haydon, P.G., 2004. Astrocytic connectivity in the hippocampus. Neuron Glia Biol. 1, 3–11.

Tamamaki, N., Yanagawa, Y., Tomioka, R., Miyazaki, J., Obata, K., Kaneko, T., 2003. Green fluorescent protein expression and colocalization with calretinin, parvalbumin, and somatostatin in the GAD67-GFP knock-in mouse. J. Comp. Neurol. 467, 60–79.

Tashiro, A., Goldberg, J., Yuste, R., 2002. Calcium oscillations in neocortical astrocytes under epileptiform conditions. J. Neurobiol. 50, 45–55.

Thomson, A.M., West, D.C., Hahn, J., Deuchars, J., 1996. Single axon IPSPs elicited in pyramidal cells by three classes of interneurones in slices of rat neocortex. J. Physiol. 496, 81–102.

Yuste, R., Katz, L.C., 1991. Control of postsynaptic Ca^{2+} influx in developing neocortex by excitatory and inhibitory neurotransmitters. Neuron 6, 333–344.

Yuste, R., Peinado, A., Katz, L.C., 1992. Neuronal domains in developing neocortex. Science 31, 665–669.